Preprints of the 19th World Congress
The International Federation of Automatic Control
Cape Town, South Africa. August 24-29, 2014

Observability Analysis on Radome Aberration Estimation

Min-Guk Seo*. Min-Jea Tahk**
Chang-Kyung Ryoo***

**Division of Aerospace Engineering, KAIST,
Daejeon, Korea, (e-mail: mgseo@fdcl.kaist.ac.kr).
** Division of Aerospace Engineering, KAIST,
Daejeon, Korea, (e-mail: mjtahk@fdcl.kaist.ac.kr).
*** Department of Aerospace Engineering, Inha University,
Incheon, Korea, (e-mail: ckryoo@inha.ac.kr).*

Abstract: The observability of radome aberration estimation with line-of-sight (LOS) angle-only measurement is studied in this paper. When missile seeker can only measure LOS angle of target, target state variables are required to be estimated with this measurement for accurate missile guidance. Since LOS angle measurement contains error, caused by radome attached at missile nose and called radome aberration angle, the state estimation performance is degenerated. Thus, the radome aberration effects should be estimated and compensated for accurate target state variable estimation. The radome aberration angle is modeled as the product of radome slope and gimbal angle. The observability of state variables and radome slope estimation is analyzed for the relative dynamics with stationary target model in polar coordinate system. Simulations are conducted to verify the observability conditions obtained in this paper.

1. INTRODUCTION

To accomplish high homing missile guidance performance, it is essential to figure out target state variables accurately. Active homing missiles obtain target state information from seeker measurement. However, when the target is equipped with anti-Electronic Counter Measures (anti-ECM), the seeker measurement is interrupted. Especially for missile with microwave seeker case, the seeker cannot measure the relative distance of target from missile, and only measures the relative direction of the target, line-of-sight (LOS) angle. Thus, target state variables are required to be estimated from LOS angle-only measurement.

Radome is a structure attached at the nose of active homing missile to protect missile seeker and reduce aerodynamic drag force acting on missile. Since missile seeker is placed inside of radome, the microwave reflected by target should pass radome to reach missile seeker. When the shape of radome is hemisphere, the microwave is not refracted by the radome, but the aerodynamic drag force is the maximum. This means that actual radome shape cannot be perfect hemisphere, so the microwave is refracted by radome. As a result, LOS angle measurement contains error, called radome aberration angle, and the target state estimation becomes inaccurate with this erroneous measurement. Thus, it is required to estimate and compensate the radome effect for high target state estimation performance.

Several radome aberration estimation methods have been developed in previous studies. Zarchan (1999) suggested a simple method using dither signal added to missile guidance command. However, due to this additional signal, homing guidance performance is able to be degraded. Neural network algorithm is introduced by Lin (2001) for radome aberration estimation. But, since its learning process is performed on the ground and the characteristics of radome changes with environment and flight conditions, it is difficult with this algorithm to accurately estimate radome aberration during actual flight. Yueh (1983, 1985), Lin (1995), and Song (2004) applied Multiple Model Filter (MMF) or Interacting Multiple Model (IMM) Filter to radome aberration estimation problem. However, those methods require a lot of models for accurate estimation. Radome slope, which is parameter representing the refraction characteristics of a certain radome, is defined as a state variable of filter algorithm by Gurfil (2004), but this algorithm requires large number of state variables for dynamic system modelling. Most of those algorithms, except for Zarchan (1999), have the same shortage that they utilize relative range between missile and target as a seeker measurement.

In this paper, the observability of radome aberration estimation with LOS angle-only measurement is analysed. The radome aberration angle is modelled with radome slope, and it is considered as a state variable. The local observability analysis method for nonlinear dynamic system based on Lie derivative and gradient operator, introduced by Hwang (1972), Bartosiewicz (1995), and Ma (2011), is utilized to derive the observable condition of the target state variables and radome aberration estimation system.

This paper is composed as follows. The observability analysis theory studied in the previous literatures is explained in Section 2. The system dynamics and measurement are modelled in Section 3. Section 4 deals with the analysis on the observability of this dynamic system. Simulation results are presented in Section 5.The conclusion of this paper is addressed in Section 6.

2. OBSERVABLE CONDITION OF NONLINEAR DYNAMIC SYSTEM

The local observability analysis method is explained in this section. An arbitrary nonlinear dynamic system with single measurement is considered as below.

$$\begin{aligned}\dot{\mathbf{x}} &= f(\mathbf{x},\mathbf{u}) \\ \mathbf{z} &= h(\mathbf{x})\end{aligned} \tag{1}$$

where $\mathbf{x} \in \Re^n$ is state variable vector and $z \in \Re^1$ is single measurement.

Two different points, $\mathbf{x} = \mathbf{x}_0$ and $\mathbf{x} = \mathbf{x}_1$, are said to be distinguishable when there exists a control input $\mathbf{u}_d$ which makes the following condition to be satisfied.

$$\mathbf{x}_0 \neq \mathbf{x}_1 \quad \Rightarrow \quad z(\mathbf{x}_0) \neq z(\mathbf{x}_1) \tag{2}$$

The dynamic system given in (1) is locally observable at $\mathbf{x}_0$ if there exists an neighbourhood of $\mathbf{x} = \mathbf{x}_0$ such that all the points included in this neighbourhood, except for $\mathbf{x} = \mathbf{x}_0$, are distinguishable from $\mathbf{x} = \mathbf{x}_0$.

To figure out the local observability condition, the Lie derivative of the given dynamic system, $l(\mathbf{x},\mathbf{u})$, is calculated as below.

$$l(\mathbf{x},\mathbf{u}) \triangleq \begin{bmatrix} h(\mathbf{x}) \\ \dot{h}(\mathbf{x}) \\ \vdots \\ h^{(n)}(\mathbf{x}) \end{bmatrix} \tag{3}$$

From the Lie derivative vector shown in (3), the gradient operator of the dynamic system, $O(\mathbf{x}_0,\mathbf{u}_d)$, is defined as

$$O(\mathbf{x}_0,\mathbf{u}_d) \triangleq \left.\frac{\partial l(\mathbf{x},\mathbf{u}_d)}{\partial \mathbf{x}}\right|_{\mathbf{x}=\mathbf{x}_0} \tag{4}$$

If the nonlinear dynamic system in (1) is locally observable at an arbitrary point $\mathbf{x}$, $O(\mathbf{x}_0,\mathbf{u}_d)$ is full-rank. This condition can be rewritten in terms of the determinant.

$$\det\left(O(\mathbf{x}_0,\mathbf{u}_d)\right) \neq 0 \tag{5}$$

3. SYSTEM MODELING

3.1 Engagement Kinematics Model

The relative engagement kinematics between missile and target is defined in 2-dimensional inertial polar coordinate system as shown in Fig. 1.

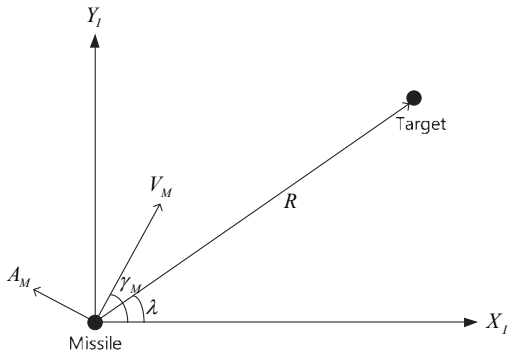

Fig. 1. Engagement Kinematics

V_M and γ_M are velocity and flight-path angle of missile, and V_M is assumed to be constant. The missile acceleration A_M is assumed to be perpendicular to the missile velocity. R stands for the relative distance between target and missile, and λ is line-of-sight(LOS) angle.

With the stationary target model, the engagement kinematics is modelled as follows.

$$\begin{aligned}\dot{\lambda} &= -\frac{1}{R}V_M \sin(\gamma_M - \lambda) \\ \dot{R} &= -V_M \cos(\gamma_M - \lambda) \\ \dot{\gamma}_M &= \frac{A_M}{V_M}\end{aligned} \tag{6}$$

3.2 Seeker Measurement Model

The relative geometry between missile seeker system with radome effect and target is shown in Fig. 2. The reference axis is defined in 2-dimensional inertial coordinate system.

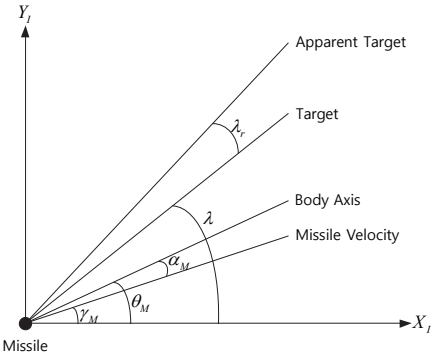

Fig. 2. Seeker Geometry

α_M and θ_M are angle-of-attack and pitch angle of missile. λ_r is radome aberration angle. Since the microwave reflected by target is refracted by radome before it reaches seeker, apparent target is detected by the seeker. This means that the LOS angle of the apparent target is measured, rather than the LOS angle of the real target. Thus, the LOS angle measurement λ_{ME} is modelled as below.

$$\lambda_{ME} = \lambda + \lambda_r \tag{7}$$

The radome aberration angle model suggested by Gurfil (2004) is defined as below.

$$\lambda_r = \rho_\theta \left(\lambda - \theta_M \right) \tag{8}$$

where ρ_θ is radome slope. With the assumption that the angle-of-attack of missile is negligible, from Fig. 2, the following relationship holds.

$$\theta_M \simeq \gamma_M \tag{9}$$

From (7), (8), and (9), the LOS angle measurement can be rewritten as

$$\lambda_{ME} = \lambda + \rho_\theta \left(\lambda - \gamma_M \right) \tag{10}$$

The radome slope is considered to be constant.

$$\dot{\rho}_\theta = 0 \tag{11}$$

4. OBSERVABILITY OF RADOME ABERRATION ESTIMATION

4.1 Nonlinear System Definition

The observable conditions of radome aberration and state variables estimation with LOS angle-only measurement is handled in this paper. This implies that the radome slope is needed to be defined as a state variable of the system. Also, the observability analysis method explained in Section 2 requires the measurement model not to include the control input. The flight path angle of missile is selected as a state variable to satisfy this measurement model requirement.

Thus, from (6), (10), and (11), the nonlinear system to analyse is defined as follows.

$$\begin{aligned} \dot{\mathbf{x}} &= f\left(\mathbf{x}, \mathbf{u}\right) \\ \mathbf{z} &= h\left(\mathbf{x}\right) \end{aligned} \tag{12}$$

where

$$\mathbf{x} = \begin{bmatrix} \lambda & R & \gamma_M & \rho_\theta \end{bmatrix}^T \qquad \mathbf{u} = A_M \tag{13}$$

$$f\left(\mathbf{x}, \mathbf{u}\right) = \begin{bmatrix} -\dfrac{1}{R} V_M \sin\left(\gamma_M - \lambda\right) \\ -V_M \cos\left(\gamma_M - \lambda\right) \\ \dfrac{A_M}{V_M} \\ 0 \end{bmatrix} \tag{14}$$

$$h\left(\mathbf{x}\right) = \left(1 + \rho_\theta\right) \lambda - \gamma_M \tag{15}$$

4.2 Observability Analysis

To analyse the observability of the dynamic system given in (12), the Lie derivative of this system is obtained from (12), (14) and (15).

$$l\left(\mathbf{x}, \mathbf{u}\right) = \begin{bmatrix} h\left(\mathbf{x}\right) \\ \dot{h}\left(\mathbf{x}\right) \\ \ddot{h}\left(\mathbf{x}\right) \\ \dddot{h}\left(\mathbf{x}\right) \end{bmatrix} \tag{16}$$

where

$$\dot{h}\left(\mathbf{x}\right) = \frac{dh\left(\mathbf{x}\right)}{dt} \quad \ddot{h}\left(\mathbf{x}\right) = \frac{d^2 h\left(\mathbf{x}\right)}{dt^2} \quad \dddot{h}\left(\mathbf{x}\right) = \frac{d^3 h\left(\mathbf{x}\right)}{dt^3} \tag{17}$$

Thus, the gradient operator $O\left(\mathbf{x}, \mathbf{u}\right)$ is derived from (16) as

$$O\left(\mathbf{x}, \mathbf{u}\right) = \begin{bmatrix} \dfrac{\partial h\left(\mathbf{x}\right)}{\partial \lambda} & \dfrac{\partial h\left(\mathbf{x}\right)}{\partial R} & \dfrac{\partial h\left(\mathbf{x}\right)}{\partial \gamma_M} & \dfrac{\partial h\left(\mathbf{x}\right)}{\partial \rho_\theta} \\ \dfrac{\partial \dot{h}\left(\mathbf{x}\right)}{\partial \lambda} & \dfrac{\partial \dot{h}\left(\mathbf{x}\right)}{\partial R} & \dfrac{\partial \dot{h}\left(\mathbf{x}\right)}{\partial \gamma_M} & \dfrac{\partial \dot{h}\left(\mathbf{x}\right)}{\partial \rho_\theta} \\ \dfrac{\partial \ddot{h}\left(\mathbf{x}\right)}{\partial \lambda} & \dfrac{\partial \ddot{h}\left(\mathbf{x}\right)}{\partial R} & \dfrac{\partial \ddot{h}\left(\mathbf{x}\right)}{\partial \gamma_M} & \dfrac{\partial \ddot{h}\left(\mathbf{x}\right)}{\partial \rho_\theta} \\ \dfrac{\partial \dddot{h}\left(\mathbf{x}\right)}{\partial \lambda} & \dfrac{\partial \dddot{h}\left(\mathbf{x}\right)}{\partial R} & \dfrac{\partial \dddot{h}\left(\mathbf{x}\right)}{\partial \gamma_M} & \dfrac{\partial \dddot{h}\left(\mathbf{x}\right)}{\partial \rho_\theta} \end{bmatrix} \tag{18}$$

After some algebraic calculations, the determinant of $O\left(\mathbf{x}, \mathbf{u}\right)$ is derived as follows.

$$\begin{aligned} &\det\left(O\left(\mathbf{x}, \mathbf{u}\right)\right) = \\ &-\frac{\left(1+\rho_\theta\right)^2 V_M^2}{R^3} \left[\dddot{\sigma} \left(\frac{2V_M}{R} \sin\sigma + \dot{\gamma}_M \right) \right. \\ &\qquad - \ddot{\sigma} \left(\frac{6V_M^2}{R^2} \sin 2\sigma + \frac{6V_M}{R} \dot{\gamma}_M \cos\sigma + \ddot{\gamma}_M \right) \\ &\qquad + \dot{\sigma} \left(\frac{12V_M^3}{R^3} \sin\sigma + \frac{2V_M}{R} \ddot{\gamma}_M \cos\sigma + \frac{12V_M^2}{R^2} \dot{\gamma}_M \right. \\ &\qquad\qquad \left. \left. + \frac{6V_M^2}{R^2} \dot{\gamma}_M \cos 2\sigma + \frac{8V_M}{r} \dot{\gamma}_M^2 \sin\sigma - \dddot{\gamma}_M^3 \right) \right] \end{aligned} \tag{19}$$

where lead angle σ is defined as

$$\sigma \triangleq \gamma_M - \lambda \tag{20}$$

During terminal homing guidance stage, the direction of missile velocity vector is almost aligned towards the target, and the magnitude of missile manoeuver required to reduce the miss distance is small. Thus, it is reasonable to assume that σ is small enough during the terminal stage, resulting in the following approximations.

$$\begin{aligned} \sin\sigma &\simeq \sigma \\ \cos\sigma &\simeq 1 \end{aligned} \tag{21}$$

From (19) and (21), observability condition determinant is approximated as

$$\det\left(O(\mathbf{x},\mathbf{u})\right) \simeq \left(1+\rho_\theta\right)^2 \frac{V_M}{R^2}\left[\left\{-\dddot{\lambda}\frac{2V_M}{R}-\dot{\gamma}_M\left(\dot{\gamma}_M\left(\ddot{\lambda}+\dot{\lambda}\frac{6V_M}{R}\right)-12\dot{\gamma}_M\dot{\lambda}^2\right)\right\}\dot{\sigma} + \left(\dddot{\lambda}+\ddot{\lambda}\frac{3V_M}{R}\right)\ddot{\sigma}-\ddot{\lambda}\dddot{\sigma}\right] \tag{22}$$

This approximated determinant in (22) becomes zero when one or more of the following conditions are satisfied.

$$\begin{aligned}&\rho_\theta = -1\\ &\dot{\lambda}(t)=0\\ &\dot{\sigma}(t)=0\\ &\dot{\gamma}_M(t)=0\end{aligned} \tag{23}$$

The value of $\det\left(O(\mathbf{x},\mathbf{u})\right)$ for each case in (23) is obtained as

$$\begin{aligned}&\rho_\theta=-1 \quad \Rightarrow \det\left(\mathbf{O}(\mathbf{x},\mathbf{u})\right)=0\\ &\dot{\lambda}(t)=0 \quad \Rightarrow \det\left(\mathbf{O}(\mathbf{x},\mathbf{u})\right)=0\\ &\dot{\sigma}(t)=0 \quad \Rightarrow \det\left(\mathbf{O}(\mathbf{x},\mathbf{u})\right)=0\\ &\dot{\gamma}_M(t)=0 \Rightarrow \det\left(\mathbf{O}(\mathbf{x},\mathbf{u})\right)=-\frac{8\left(1+\rho_\theta\right)^2 V_M^6}{R^7}\sin^4\sigma\end{aligned} \tag{24}$$

Thus, from (5) and (24), the dynamic system defined in (12) is locally observable at an arbitrary point $\mathbf{x}$ when all of the following observability conditions are satisfied.

$$\begin{aligned}&a)\quad \rho_\theta \neq -1\\ &b)\quad \dot{\lambda}(t)\neq 0\\ &c)\quad \dot{\sigma}(t)\neq 0\end{aligned} \tag{25}$$

As shown from (5) and (24), $\dot{\gamma}_M(t)\neq 0$ is not a necessary condition for the local observability of the system given in (12) at an arbitrary point $\mathbf{x}$. However, since (19) becomes 0 when $\dot{\gamma}_M(t)=\sigma=0$ and (22) equals to 0 for $\dot{\gamma}_M(t)=0$ case, the state estimation performance with the dynamic model in (12) is expected to be low for non-maneuvering missile, $\dot{\gamma}_M(t)=0$, in small lead angle case.

5. SIMULATION

In order to verify the local observability conditions derived in Section 4, state variables and radome aberration estimation simulations are performed. The estimatior is designed by applying Extended Kalman Filter (EKF) algorithm to the dynamic system in (12). The target is considered to be stationary.

The initial position and velocity of missile and target are given in inertial Cartesian coordinate system as

$$\begin{aligned}&\left[X_M \quad Y_M\right]^T=\left[0 \quad 0\right]^T(m)\\ &\left[V_{M_X} \quad V_{M_Y}\right]^T=\left[600 \quad 0\right]^T(m/sec)\\ &\left[X_T \quad Y_T\right]^T=\left[10000 \quad 1000\right]^T(m)\end{aligned} \tag{26}$$

From (26), the actual initial state vector is obtained as below.

$$\mathbf{x}_0=\left[\lambda \quad R \quad \gamma_M \quad \rho_\theta\right]^T_{t=0}=\left[5.7106^\circ \quad 10050m \quad 0^\circ \quad 0.02\right]^T \tag{27}$$

The initial guess of state vector and covariance matrix are defined to be

$$\hat{\mathbf{x}}_0=\left[7.7106^\circ \quad 12050m \quad 2^\circ \quad 0\right]^T \tag{28}$$

$$\hat{\mathbf{P}}_0=\mathrm{diag}\left[0.5(\deg)^2 \quad 500^2m^2 \quad 0.5(\deg)^2 \quad 0.5^2\right] \tag{29}$$

The actual radome slope is selected as

$$\rho_\theta = 0.02 \tag{30}$$

The transfer function from missile acceleration A_M to missile pitch angle θ_M is expressed with turning rate time constant, T_α.

$$\frac{\dot{\theta}_M(s)}{A_M(s)}=\frac{1}{V_M}\left(1+T_\alpha s\right), \qquad T_\alpha=1.0sec \tag{31}$$

The missile autopilot system is modelled as 1st-order lag system by introducing time constant τ as below.

$$\frac{A_M(s)}{A_{cmd}(s)}=\frac{1}{\tau s+1}, \qquad \tau=0.1sec \tag{32}$$

where A_{cmd} is missile acceleration command.

Two different guidance algorithms, Proportional Navigation Guidance (PNG) law and Adaptive Intermittent Maneuver (AIM), are utilized to generate missile guidance command. AIM is designed by Lee (2001) in order to maintain LOS angle rate to be larger than a certain level during flight. The design parameters of guidance laws are defined as below.

$$\begin{aligned}&N_{PNG}=4\\ &N_{AIM}=2\\ &k=0.5\\ &\mu_U=0.0001741\\ &\mu_L=0.00008705\end{aligned} \tag{33}$$

where $N_{(\bullet)}$ is the navigation ratio of each guidance algorithm.

The simulation is performed as an open-loop test, meaning that the guidance command is generated by the true state variable values, not the estimated ones. The following results are accomplished by utilizing Monte-Carlo method with 100 times of simulation runs for each guidance law case.

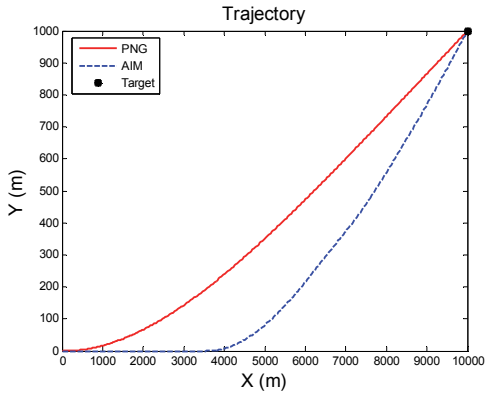

(a) Missile Trajectory

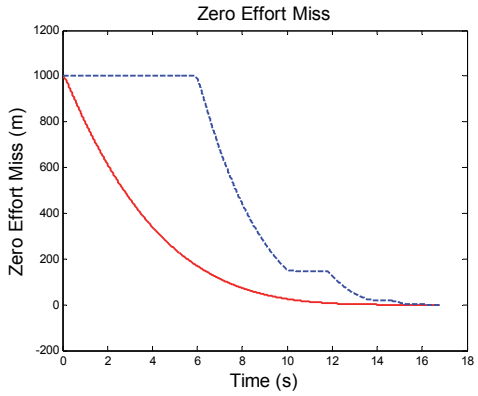

(b) Zero-Effort-Miss Distance

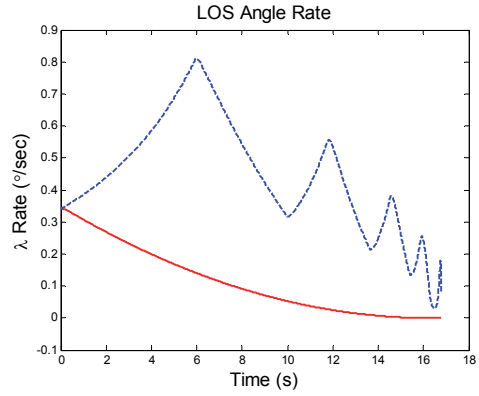

(c) LOS Angle Rate History

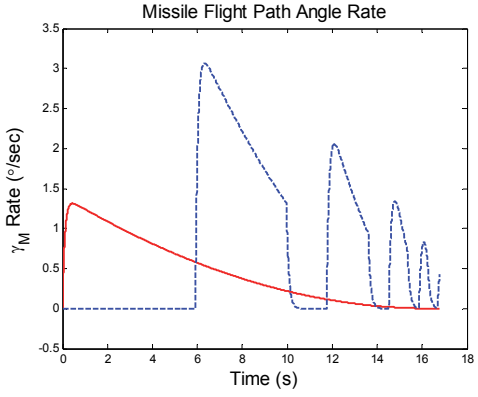

(d) Flight Path Angle Rate History

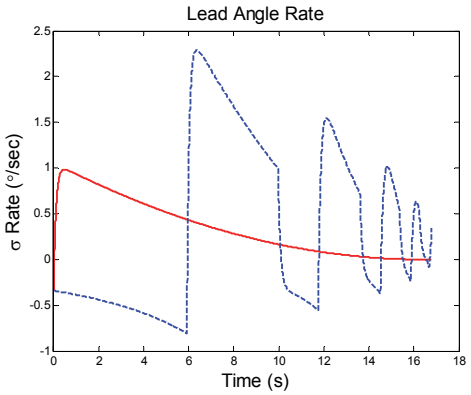

(e) Lead Angle Rate History

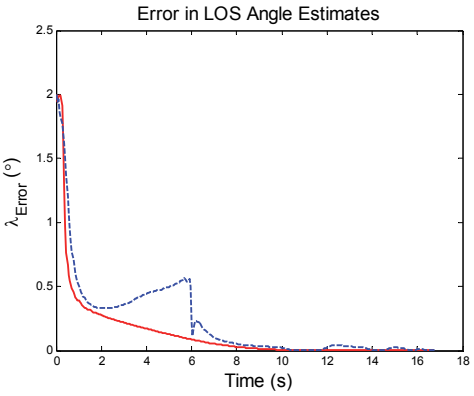

(f) LOS Angle Estimation Error

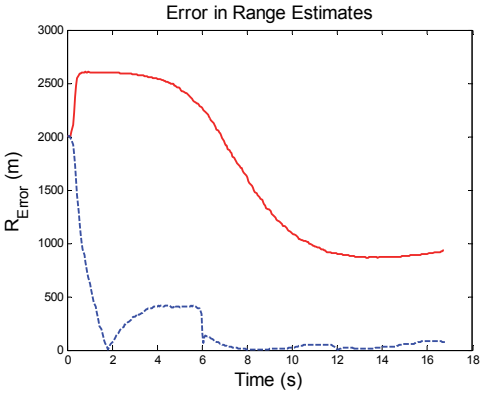

(g) Relative Range Estimation Error

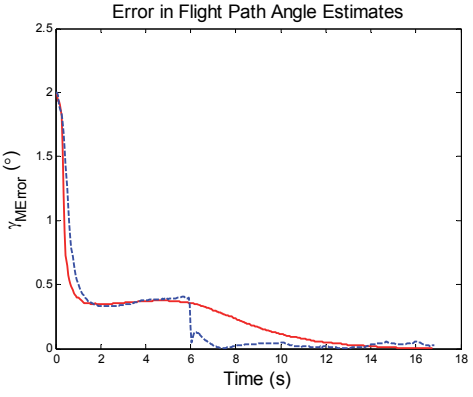

(h) Missile Flight Path Angle Estimation Error

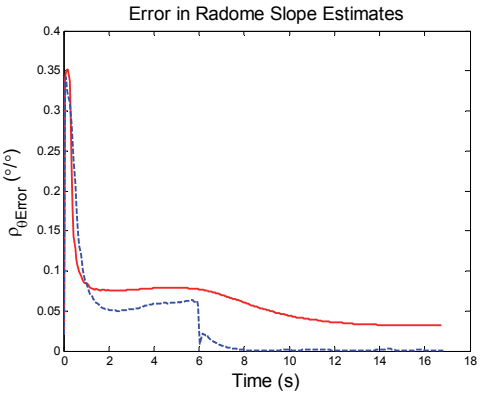

(i) Radome Slope Estimation Error

Fig. 3. State Variables and Radome Aberration Estimation

As shown in Fig. 3-(f) and (h), the estimation errors of LOS angle and missile flight path angle in both guidance law cases converge to zero as missile approaches target. However, it is given in Fig. 3-(g) and (i) that the estimation errors of relative range and radome slope in PNG law case are significantly larger than those in AIM case.

When missile guidance command is generated from PNG law, LOS angle rate monotonically converges to 0 as missile approaches target. Also, missile acceleration command is proportional to LOS angle rate in this case, and missile flight path angle rate is proportional to missile acceleration, as shown in (6). Thus, missile flight path angle rate also diminishes to 0 as LOS angle rate gets smaller. Lead angle rate is a difference between missile flight path angle rate and LOS angle rate, so its magnitude also decreases. Those characteristics are addressed in Fig. 3-(c), (d), and (e). Thus, it is shown from simulation results in Fig. 3-(c), (d), and (e) that PNG law drives the system to violate the local observability conditions defined in (25), resulting in low estimation performance as shown in Fig. 3-(g) and (i).

On the other hand, in AIM case, the magnitude of LOS angle rate is maintained to be larger than certain curve. Missile flight path angle rate has non-zero value when guidance command is generated, except for the time when missile does not maneuver. As a result, lead angle rate does not converge to 0 . Those trends are also shown in Fig. 3-(c), (d), and (e), and these results mean that the guidance command calculated from AIM make the system to satisfy the local observability conditions in (25). The simulation results in Fig. 3-(f), (g), (h), and (i), where the estimation performance in the AIM case is shown to be superior to that of the PNG law case, support this argument. However, since the estimation errors in AIM case is large at the early stage, the time interval when missile does not maneuvers and flight path angle rate is 0 , a guidance algorithm to enhance the observability during this period is required to be developed.

6. CONCLUSION

The observability analysis of radome aberration and target state estimation with LOS angle-only measurement is handled in this paper. The engagement kinematics is defined in 2-dimensional polar coordinate system and the radome aberration angle is modelled with the parameter called radome slope. The local observability conditions are derived by applying the observability analysis method based on the ful-rank condition of gradient operator derived from Lie derivatives. Simulation results imply that the obtained observability conditions on state variables are related to the radome aberration and target state estimation performance, and it is shown that time histories of state variables are considerably affected by guidance laws. Thus, it is necessary to introduce a guidance law which can guarantee the observability of the radome slope estimation.

REFERENCES

Zarchan, P., and Gratt, H. (1999). Adaptive Radome Compensation using Dither. *Journal of Guidance, Control, and Dynamics,* **22(1)**, 51-57.

Lin, C. L. (2001). Stability Analysis of Radome Error and Calibration Using Neural Networks. *IEEE Transactions on Aerospace and Electronic Systems,* **37(4)**, 1442-1450.

Yueh, W. R. (1983). Adaptive Estimation Scheme for Radome Error Calibration. *In Decision and Control, 1983. The 22nd IEEE Conference on,* **22**, 546-551.

Yueh, W. R., and Lin, C. F. (1985). Guidance Performance Analysis with In-Flight Radome Error Calibration. *Journal of Guidance, Control, and Dynamics,* **8(5)**, 666-669.

Lin, J. M., and Chau, Y. F. (1995). Radome Slope Compensation using Multiple-Model Kal-man Filters. *Journal of Guidance, Control, and Dynamics,* **18(3)**, 637-640.

Song, T. L., Lee, D. G., and Shin, S. J. (2005). Active homing performance enhancement with multiple model radome slope estimation. *Proceedings of the Institution of Mechanical Engineers, Part G: Journal of Aerospace Engineering,* **219(3)**, 217-224.

Gurfil, P. and Kasdin, N. J. (2004). Improving missile guidance performance by in-flight two-step nonlinear estimation of radome aberration. *IEEE Transactions on Control System Technology,* **12(4),** 532-541.

Hwang, M. and Seinfeld, J. H. (1972). Observability of nonlinear systems. *Journal of Optimization Theory and Applications,* **10(2),** 67-77.

Bartosiewicz, Z. (1995). Local observability of nonlinear systems. *Systems & Control Letters,* **25(4),** 295-298.

Ma, Q. (2011). Structural Conditions on Observability of Nonlinear Systems. *International Journal of Information Technology and Computer Science,* **3(4),** 16-22.

Lee, H. I., Tahk, M. J., and Sun, B. C. (2001). Practical dual-control guidance using adaptive intermittent maneuver strategy. *Journal of Guidance, Control, and Dynamics,* **24(5)**, 1009-1015.